

**Mathematical Considerations of Antiretroviral  
Therapy Aimed at HIV-1 Eradication or  
Maintenance of Low Viral Loads**

Wein, D'Amato, and Perelson

#3939-97-MSA

February, 1997

# Mathematical Considerations of Antiretroviral Therapy Aimed at HIV-1 Eradication or Maintenance of Low Viral Loads

*Lawrence M. Wein*

Sloan School of Management, M.I.T.  
Cambridge, MA 02139

*Rebecca M. D'Amato*

Operations Research Center, M.I.T.  
Cambridge, MA 02139

*Alan S. Perelson*

Theoretical Division, Los Alamos National Laboratory  
Los Alamos, NM 87545

## Abstract

**Objectives:** To investigate factors that may influence the success or failure of powerful antiretroviral regimens to eradicate HIV-1 or to maintain viral loads at low levels.

**Methods:** A mathematical model is constructed that tracks the dynamics of CD4<sup>+</sup> T cells, a population of cells that remains long-lived when productively infected by HIV-1, and two viral strains (wild-type and drug-resistant mutant), under a combination regimen of reverse transcriptase and protease inhibitors. A mathematical analysis of the long-term (steady-state) and short-term (transient) behavior of the model is undertaken, and various scenarios are illustrated.

**Results:** The transient behavior of the cells and virus and the eventual eradication of the virus are dictated by two factors: the strength of the combination therapy and the maximum achievable increase in the uninfected CD4<sup>+</sup> T cell concentration. A simple formula is given which suggests under what conditions eradication might occur.

**Conclusions:** For eradication to occur, therapy needs to be nearly as efficacious (roughly 60-90% of potential infectious virus production needs to be blocked) against mutant strains of virus as it is against the wild-type strain. The eradication condition for maintenance therapy is the same as the eradication condition for induction therapy, despite the fact that induction therapy is apt to be faced with a higher viral load. If induction therapy is unable to achieve eradication then the steady-state viral load and CD4<sup>+</sup> T cell count resulting from maintenance therapy are independent of the timing of the switch to maintenance therapy. Drug therapy is unlikely to maintain viral loads at low levels; it is apt to either eradicate the virus or allow the viral load to return to near its pre-treatment level.

**Keywords:** Antiretroviral therapy, drug resistance, mathematical models

## Introduction

Combinations of reverse transcriptase (RT) and protease inhibitors have succeeded in suppressing the level of human immunodeficiency virus of type 1 (HIV-1) in the plasma of HIV-1 infected individuals to below the current threshold of detection [1, 2, 3]. While the great majority of HIV-1-infected patients experience sustained viral suppression on these potent drug regimens, initial indications suggest that after one year the HIV RNA becomes detectable in the plasma in roughly 10% of patients adhering to a combination antiretroviral regimen [1]. This observation raises the following questions: What causes the failure of these powerful combinations of agents? For patients that maintain viral suppression, what happens if they are switched from the powerful multidrug *induction* therapy to a less intensive *maintenance* therapy [4], in an attempt to reduce cost, toxicity and possible noncompliance? Perhaps most importantly, in patients with sustained suppression of virus, can the virus eventually be eradicated by induction and maintenance therapies? This paper develops and analyzes mathematical models to address these three questions. Because the model is not tested against data, our results should be regarded cautiously.

A number of mathematical models have already been developed to describe the population dynamics of HIV-1 following drug treatment and the emergence of drug-resistant mutants [5]-[16]. Our model follows the general strategy of this previous work but incorporates new data suggesting that to characterize the effects of drug therapy for longer than a few weeks one needs to consider the infected  $CD4^+$  T cells plus other reservoirs of HIV-1 [3]. After potent antiretroviral therapy is initiated in HIV-1-infected patients, the concentration of HIV-1 RNA measured in plasma exhibits an initial rapid exponential decline of nearly 2-logs (first phase) during the first two weeks of treatment, followed by a slower exponential decline (second phase) which over the course of weeks to months lowers the viral load to an undetectable level [3]. The first, rapid phase of decline has been observed in a number of

studies [5, 6, 7, 17] and is due to the loss of productively infected  $CD4^+$  T cells [3, 7]. The slower, second phase of decline may reflect the loss of cells, such as macrophages, which were infected prior to treatment but which may live and produce HIV-1 for many weeks, the slow activation of latently infected cells into productive infection or the release of virions trapped in lymphoid tissue. A simultaneous analysis of both plasma viremia and the kinetics of decay of HIV infection in peripheral blood mononuclear cells suggests that the activation of latently infected cells is not a major source of HIV-1 during the second phase of viral decline and can be ignored when compared with the contribution of virus from other sources [3].

### The Model

Our mathematical model builds on the “long-lived infected cell” model, recently developed by Perelson *et al.* [3], which can account in a quantitatively accurate manner for both the first and second phases of viral decline. As in their model, we consider  $CD4^+$  T cells, denoted by  $T$ , which are short-lived after becoming productively infected, and a second compartment, denoted by  $M$ , which is a long-lived source of virus. The second compartment may be long-lived productively infected cells, such as macrophages, dendritic cells or a combination of these plus other cell types, or a pool of virions trapped in lymphoid tissue that decays and slowly leaks virions out into the plasma. For simplicity, we will refer to the second compartment as a long-lived pool of cells, and occasionally as “macrophages”, but as of yet there is no conclusive evidence to support this interpretation.

Our model generalizes the model in [3] in three ways. First, it includes a drug-sensitive wild-type strain and a drug-resistant mutant strain of virus, which are referred to as strains 1 and 2, respectively; to minimize confusion, the subscripts 1 and 2 are used to index the virus strains, and the superscript  $M$  is used to denote parameters that are related to the long-lived pool of cells. In the absence of therapy and mutations, infectious virus of

strain  $i$ ,  $V_i^I$ , infects  $CD4^+$  cells at rate  $k_i$  and causes them to become productively infected cells,  $T_i^*$ , and infects long-lived cells at rate  $k_i^M$  and transforms them into productively infected cells,  $M_i^*$ . However, due to errors in reverse transcription, we assume that reverse transcription of strain  $i$  results in cells infected by strain  $j$  at the mutation probability  $m_{ij}$ , where  $m_{ii}$  is the frequency of error-free transcription. In this first model, we do not consider the stepwise accumulation of mutations. Thus the mutation probability  $m_{12}$  is the probability that wild-type virus is transformed into a partially drug-resistant mutant strain during reverse transcription. Productively infected cells  $T_i^*$  and  $M_i^*$  are lost at per capita rate  $\delta_i$  and  $\delta_i^M$ , respectively, and produce virions at rate  $\pi_i = N_i\delta_i$  and  $\pi_i^M = N_i^M\delta_i^M$  per cell, respectively, where  $N_i$  and  $N_i^M$  are the total number of virions (the burst size), respectively, produced during their lifetimes.

Our second generalization of the model in [3] is the incorporation of a combination of RT and protease inhibitors that is not 100% effective, particularly against the mutant virus. Although our analysis can incorporate differential drug efficacies, we assume the same efficacy against the different cell populations because of the lack of data on this issue and because the analytical results are more transparent in this case. For  $i = 1, 2$ , let  $r_i$  denote the fraction of new cell infections by virus strain  $i$  that are blocked by the RT inhibitors in the drug regimen, and let  $p_i$  denote the fraction of newly produced virions of strain  $i$  that are rendered noninfectious by the protease inhibitors. Here we envision all virus as being part of an infectious pool unless it is rendered noninfectious by a protease inhibitor. The values of  $r_i$  and  $p_i$  will depend on the drug dose administered, as well as the sensitivity of the viral strains to the drugs. The inclusion of protease inhibitors in the model forces us to distinguish between infectious and noninfectious pools of virus; we let  $V_i$ ,  $i = 1, 2$ , denote the total (infectious plus noninfectious) concentration of virions of strain  $i$ ,  $V_i^I$  denote the concentration of infectious virus of strain  $i$ , and  $V$  denote the total viral load. For modeling

purposes, we assume that all virus is infectious (i.e., part of an infectious pool of virions) before treatment is initiated. Both infectious and noninfectious virus of strain  $i$  are assumed to be cleared at rate  $c_i$ .

The final generalization with respect to [3] is the incorporation of the dynamics of the uninfected cell populations,  $T$  and  $M$ . The uninfected cells have a natural death rate of  $\mu$  and  $\mu^M$ , respectively, in addition to the loss that is experienced by viral infection. Uninfected long-lived cells are produced from a pool of precursors at constant rate  $\lambda^M$ . Uninfected CD4<sup>+</sup> T cells are produced from precursors in the thymus at rate  $s$ ; we assume that this source of new cells is small compared with their proliferation and can be ignored. In the model, CD4<sup>+</sup> T cells proliferate exponentially at a rate that follows a logistic growth function (see Figure 2b of [6]), with a maximum rate of  $\lambda$  and a maximum uninfected CD4<sup>+</sup> concentration of  $T_{\max}$ . Because we use the model to study events after combination therapy has begun,  $T_{\max}$  refers to the maximum uninfected CD4<sup>+</sup> concentration that can be obtained in a patient whose immune system may already be damaged through HIV infection. Thus,  $T_{\max}$  may be lower than the T cell count in an healthy, HIV-1 uninfected person. The model is summarized in Figure 1 and the system of equations describing it are given in the Appendix.

The model omits latently infected cells, which do not appear to play a big role [3], and assumes that the strength of the immune response does not change over the time period under study. We also assume that the plasma and the lymph system are in equilibrium [18], and thus that measurements of viral load in plasma are indicative of the HIV-1 concentration in extracellular fluids throughout the body.

This model is analyzed mathematically and solved numerically below. Table 1 contains parameter values that are used in the numerical studies; see the Appendix for a derivation of these values.

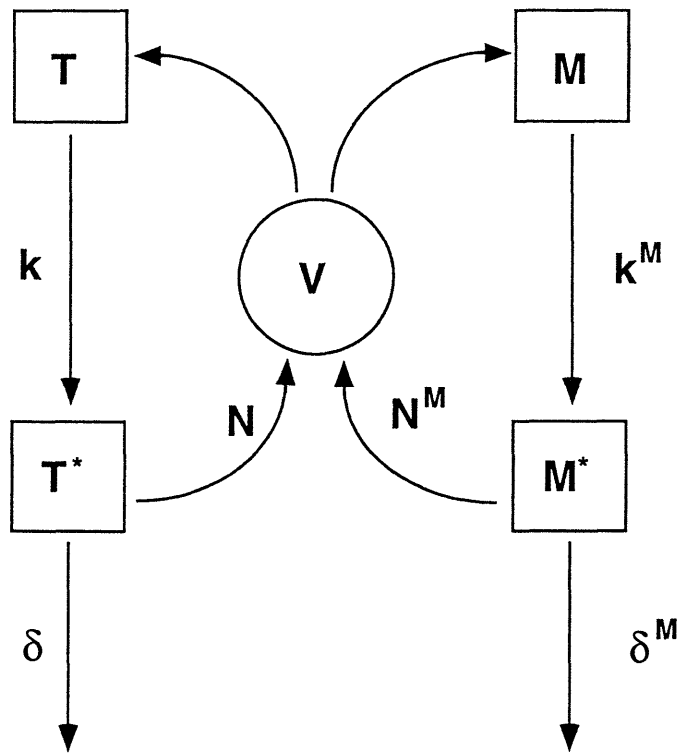


Figure 1: Schematic diagram of the model. Virus,  $V$ , infects  $CD4^+$  T cells,  $T$ , with rate constant  $k$  and generates productive infected T cells,  $T^*$ . The virus also infects long-lived cells,  $M$ , with rate constant  $k_M$  and produces productively infected long-lived cells,  $M^*$ . Productively infected T cells,  $T^*$ , die at per capita rate  $\delta$  and produce a total of  $N$  virions during their lifetime. Thus the average rate of virion production is  $\pi = N\delta$ . Analogously, productively infected long-lived cells,  $M^*$ , die at per capita rate  $\delta^M$  and produce a total of  $N^M$  virions at an average rate of  $\pi^M = N^M\delta^M$ . In the full model, described in the Appendix, uninfected  $CD4^+$  T cells are renewed by proliferation, whereas uninfected long-lived cells are renewed at a constant rate from precursors. Both populations of uninfected cells have finite lifespans and die at rate  $\mu$  and  $\mu^M$ , respectively. The full model also considers two classes of virus, drug-sensitive wild-type,  $V_1$ , and partially drug-resistant mutant,  $V_2$ . After protease inhibitors are given some virus is rendered noninfectious. Thus wild-type and mutant virus are further classified as “infectious” (i.e. protease not inhibited) or “noninfectious” (i.e. protease inhibited).



Variables		Initial Values
$T$	Uninfected CD4 <sup>+</sup> cells	178.81 cells mm <sup>-3</sup>
$T_1^*$	CD4 <sup>+</sup> cells infected by strain 1	1.19 cells mm <sup>-3</sup>
$T_2^*$	CD4 <sup>+</sup> cells infected by strain 2	0.004 cells mm <sup>-3</sup>
$M$	Uninfected macrophages	49.2 cells mm <sup>-3</sup>
$M_1^*$	Macrophages infected by strain 1	0.49 cells mm <sup>-3</sup>
$M_2^*$	Macrophages infected by strain 2	1.7 × 10 <sup>-3</sup> cells mm <sup>-3</sup>
$V_1^I, V_1$	Virus of strain 1 (infectious, total)	133.55 10 <sup>3</sup> virions ml <sup>-1</sup>
$V_2^I, V_2$	Virus of strain 2 (infectious, total)	0.45 10 <sup>3</sup> virions ml <sup>-1</sup>
Parameters		Values
$s$	Rate of supply of uninfected CD4 <sup>+</sup> cells	0
$\lambda$	Max. growth rate of uninfected CD4 <sup>+</sup> cells	0.01 day <sup>-1</sup>
$T_{\max}$	Maximum uninfected CD4 <sup>+</sup> cells	450 cells mm <sup>-3</sup>
$\mu$	Death rate of uninfected CD4 <sup>+</sup> cells	0.0014 day <sup>-1</sup>
$\delta_1, \delta_2$	Loss rates of infected CD4 <sup>+</sup> cells	0.69 day <sup>-1</sup>
$k_1, k_2$	Infectivity rates of virus	3.43 × 10 <sup>-5</sup> ml 10 <sup>-3</sup> virions <sup>-1</sup> day <sup>-1</sup>
$N_1$	Burst size of strain 1	480.1 virions cell <sup>-1</sup>
$N_2$	Burst size of strain 2	475.3 virions cell <sup>-1</sup>
$c_1, c_2$	Death rates of virus	3.07 day <sup>-1</sup>
$m_{12}, m_{21}$	Mutation probabilities	3.4 × 10 <sup>-5</sup>
$\lambda^M$	Production rate of uninfected macrophages	2.0 cells mm <sup>-3</sup> day <sup>-1</sup>
$\mu^M$	Death rate of uninfected macrophages	0.04 day <sup>-1</sup>
$\delta_1^M, \delta_2^M$	Loss rates of infected macrophages	0.062 day <sup>-1</sup>
$k_1^M, k_2^M$	Infectivity rates of virus	4.67 × 10 <sup>-6</sup> ml 10 <sup>-3</sup> virions <sup>-1</sup> day <sup>-1</sup>
$N_1^M$	Burst size of strain 1 from macrophages	534.4 virions cell <sup>-1</sup>
$N_2^M$	Burst size of strain 2 from macrophages	529.0 virions cell <sup>-1</sup>

Table 1. Parameter values for the model. See the Appendix for a derivation of these values.

## Eradication

We assume that a potent antiviral regimen is applied to an HIV-1-infected patient starting at time zero. This will cause a change in the viral load and eventually either a new steady state will be reached or the virus will be eradicated. The eradication of the virus is indicated by a post-treatment steady state in which the viral load is zero. We perform a steady-state analysis and a dynamic analysis.

**Post-treatment steady-state results.** We consider the following question: If the drug regimen is very effective against the wild-type virus but not against the mutant virus, then under what conditions will all the virus eventually be eliminated? Define the *drug efficacy* of the combination therapy against virus strain  $i$  to be

$$e_i = 1 - (1 - r_i)(1 - p_i). \quad (1)$$

In the model, a fraction  $1 - r_i$  of potential viral infections is not blocked by the RT inhibitors and, of the new virus produced by these infections, a further fraction  $1 - p_i$  is rendered noninfectious by the protease inhibitors. Hence,  $e_i$  is the fraction of potential infectious virus production in our model that is blocked by the antiretroviral regimen.

To determine the condition for eradication of the virus, we employ several assumptions that simplify both the mathematical analysis and the mathematical results. For example, in our mathematical analysis we assume that the drug regime is 100% effective against the wild-type virus (i.e.,  $r_1 = p_1 = 1$ ). In numerical investigations we relax the simplifying assumptions; for example, we may assume that the drug regime is only close to being fully effective (e.g.  $r_1 = 0.9$ ,  $p_1 = 0.99$ ). Our numerical investigations indicate that the mathematical results reported here are typically within several per cent of the exact (and much more complex) mathematical results across a wide range of parameter values. A statement of the simplifying assumptions and the ensuing mathematical analysis can be found in the Appendix.

Our main mathematical result is that the virus is eradicated if the drug efficacy against the resistant virus,  $e_2$ , obeys the following inequality:

$$e_2 > 1 - \frac{\lambda c_2}{(\lambda - \mu)k_2 N_2 T_{\max}}, \quad (2)$$

derived from Eq. (27) in the Appendix. Because we have assumed that the drug regime is 100% effective against the wild-type virus,  $e_1 = 1$  and this parameter does not enter into the condition for eradication. This equation predicts that resistant strains that have high virulence (interpreted here as having a high value of the infectivity rate constant  $k_2$  or large burst size  $N_2$ ), will be more difficult to eradicate than less virulent strains; the drug efficacy,  $e_2$ , needs to be higher to eradicate strains with larger values of  $k_2 N_2$ .

The inequality (2) can be rewritten in terms of other more directly measured parameters by assuming that before treatment is initiated patients are in quasi-steady-state and very little mutant virus is present. Then setting equations (15) and (20) in the Appendix to zero gives the equations  $k_1 T(0) V_1^I(0) = \delta_1 T_1^*(0)$  and  $N_1 \delta_1 T_1^*(0) = \eta c_1 V_1^I(0)$ , where we have assumed that a fraction  $\eta$  of the newly produced virus is generated by productively-infected CD4<sup>+</sup> T cells. Eliminating  $\delta_1 T_1^*(0)$  from these two equations gives  $k_1 N_1 T(0) = \eta c_1$ . If we assume that the clearance rate of both wild-type and mutant strains is identical (i.e.,  $c_1 = c_2$ ) and let  $f = k_2 N_2 / (k_1 N_1)$ , then equation (2) reduces to

$$e_2 > 1 - \left( \frac{1}{\eta f} \frac{\lambda}{\lambda - \mu} \right) \frac{T(0)}{T_{\max}}. \quad (3)$$

The parameter  $f = k_2 N_2 / (k_1 N_1)$  can be considered as a measure of the *relative fitness* of the mutant virus, although it is not the usual ratio of Malthusian parameters used in the formal population genetics definition [19].

The inequality (3) can also be expressed in terms of the total CD4<sup>+</sup> T cell count rather than the concentration of uninfected CD4<sup>+</sup> cells,  $T$ . For example, if we consider a patient who before treatment has roughly 5% of his CD4<sup>+</sup> cells infected [20] then  $CD4^+(0) = 1.05 T(0)$ . If the concentration of uninfected CD4<sup>+</sup> T cells ever reaches  $T_{\max}$  then presumably very few cells will be infected, and we can assume  $CD4_{\max}^+ = T_{\max}$ . Furthermore, the maximum proliferation rate  $\lambda$  of CD4<sup>+</sup> T cells is much larger than the natural death rate  $\mu$  [21]. Using

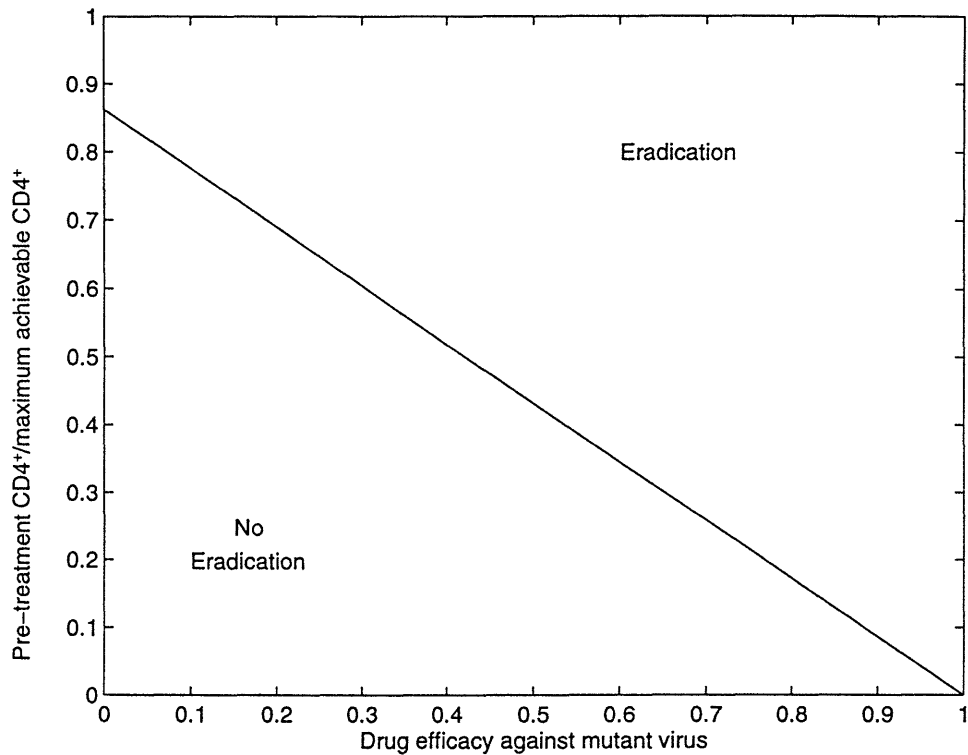


Figure 2: The virus eradication condition depends primarily on the efficacy of the drug combination against the mutant virus,  $e_2$ , and the ratio of the pre-treatment  $CD4^+$  cell count to the maximum achievable  $CD4^+$  cell count. As in equation (4), we set  $\lambda/(\lambda - \mu) = 1.16$ ,  $\eta = 0.96$  [3], and  $f = 0.99$ .

the parameter values in Table 1,  $\lambda/(\lambda - \mu) = 1.16$ ,  $\eta = 0.96$  [3], and assuming that the mutant virus is only slightly less fit than the wild-type virus,  $f = 0.99$  [22], we find that the virus is eradicated if

$$e_2 > 1 - 1.16 \frac{CD4^+(0)}{CD4^+_{\max}}. \quad (4)$$

The constant 1.16 depends on our choice of parameters but in general will be somewhat greater than one. For example, if the mutant virus were only 90% as fit as the wildtype virus, i.e.  $f = 0.9$ , then the constant 1.16 would be replaced by 1.28.

From (4) and Figure 2, we see that the condition for eradication depends mainly on the drug efficacy against the mutant virus,  $e_2$ , and the ratio of the pre-treatment  $CD4^+$  count to the maximum achievable  $CD4^+$  count; other factors determine the constant 1.16.

Not surprisingly, the more efficacious the drug regimen is against the mutant virus, i.e., the higher  $e_2$ , the easier it is to eradicate the virus. Less intuitive is the observation that the larger the value of  $CD4^+_{max}$ , the larger the potential pool of uninfected  $CD4^+$  T cells, and the more difficult it is to eradicate the virus.

The ratio  $CD4^+(0)/CD4^+_{max}$  is likely to vary significantly among HIV-infected individuals. An upper bound on this ratio can be determined by observing the increase in  $CD4^+$  counts during combination therapy. For 30 patients on triple combination therapy for 48 weeks [1], the means were  $CD4^+(0)=142$  and  $CD4^+(48)=360$ , which gives an estimated lower bound for the critical value of  $e_2$  in (4) of 0.54 (although the ratio of the means is not equal to the mean of the ratios). This aggregate calculation suggests that the drug efficacy against the mutant virus must be at least 0.54 for eradication to occur.

The steady-state total viral load,  $V$ , and the steady-state  $CD4^+$  count, are plotted versus the drug efficacy against the mutant virus,  $e_2$ , in Figure 3, using the parameter values in Table 1. The viral load is relatively insensitive to the drug efficacy for the resistant virus until  $e_2$  approaches the eradication threshold (Fig. 3). Hence, except for a very narrow window for the drug efficacy parameter, the drug regimen will either achieve viral eradication or an essentially fixed viral load. A similar conclusion has been reached by Bonhoeffer, Coffin and Nowak [23] using a different model of HIV dynamics. The post-treatment steady state  $CD4^+$  count increases with the drug efficacy in a convex manner until the virus is eradicated; thereafter, the  $CD4^+$  count is constant.

While our model was designed to examine the treatment consequences of combination therapy, it can also be used to study treatments involving only RT inhibitors or only protease inhibitors. Clinical trials using the RT inhibitors AZT and 3TC have shown that, unlike the predictions made above, the viral load neither goes undetectable nor goes back to its pre-treatment steady-state value. Rather, under long-term AZT-3TC treatment a new steady

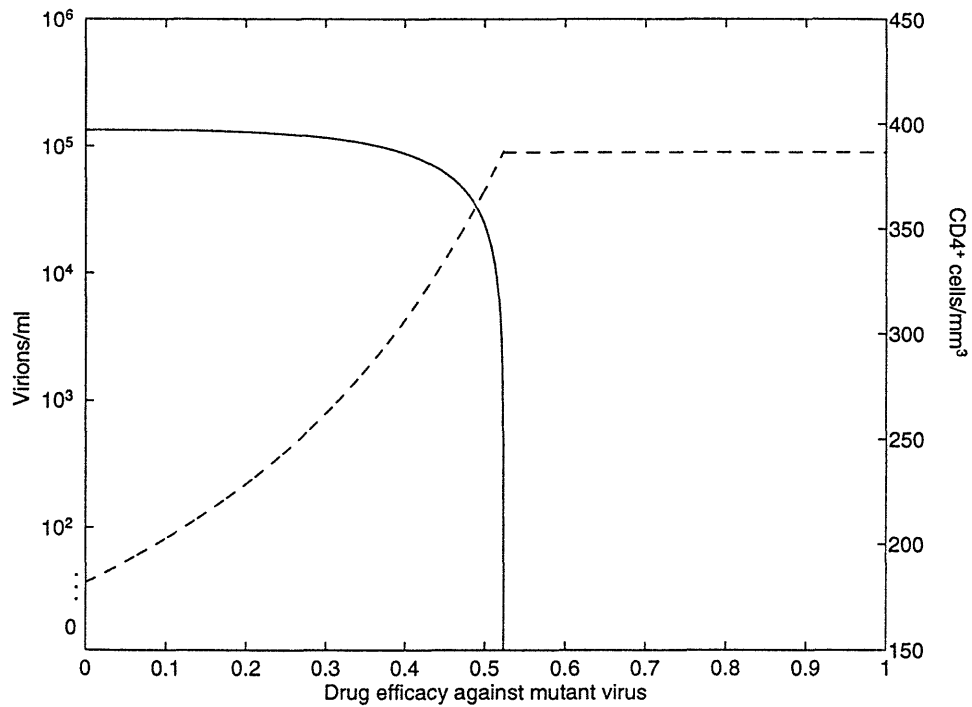


Figure 3: The steady-state viral load (solid line),  $V$ , and the steady-state CD4<sup>+</sup> T cell count (dashed line) plotted as a function of the drug efficacy,  $e_2$ , against the mutant virus. The curves were computed under the assumption that the drug regime is 100% effective against wild-type virus so that at steady state,  $V_1 = 0$ , and all virus present is mutant. In this example, the threshold is  $e_2 = 0.523$ , which is computed in the Appendix to more precision than given by equation (4).

state viral load is obtained that is 10-100 fold lower than the pre-treatment steady state [24]. However, as shown in Table 2, a steady state in which the viral load is diminished say 10-fold (i.e.  $V_2 = 0.1V(0)$ ) when a combination of RT inhibitors is given can be obtained from our model with a variety of parameter choices describing the relative fitness of the mutant,  $f$ , and the effectiveness of the drug combination on the mutant,  $r_2$ .

$r_2$	$f$
0.15	0.581
0.25	0.655
0.35	0.752

Table 2. Some parameter combinations for the effectiveness of the RT inhibitors on the mutant,  $r_2$ , and the relative fitness of the mutant,  $f$ , that lead to a post-treatment steady state that is 10-fold lower than baseline. All unlisted parameters have values as defined in Table 1.

**Dynamic results.** Our objective is to understand the transient behavior of the model after a drug perturbation is given. We are particularly interested in the rate of growth of mutant virus in the case where eradication does not occur. Our mathematical analysis is presented in the Appendix; here we only describe the salient features of the results.

If we assume that the drug efficacy against the wild-type virus is 100% ( $r_1 = 1$ ,  $p_1 = 1$ ) and ignore the small contribution from any back mutation from mutant to wild-type, then the wild-type viral load after therapy is initiated,  $V_1(t)$ , given by equation (2) in [3], exhibits a biphasic decay. The first, rapid phase of viral decline lasts for several weeks and is due to the loss of productively infected  $CD4^+$  T cells. This is then followed by a second, slow phase of decline due to the loss of productively infected long-lived cells.

To calculate the dynamics for the mutant virus,  $V_2(t)$ , we need only assume that the protease inhibitors are 100% effective against the wild-type virus ( $p_1 = 1$ ), but can allow the RT inhibitors to be imperfect at blocking wild-type viral infections. Further, we make two important assumptions to simplify the analysis: First, we ignore the long-lived cells. Mathematical and numerical investigations of the problem including long-lived cells reveal

that these long-lived cells have little effect on the dynamics when eradication does not occur. Second, as in [3, 5, 6, 7], we assume that the uninfected CD4<sup>+</sup> concentration  $T(t)$  remains at its pre-treatment steady state value,  $T(0)$ ; as a consequence, our analysis is only valid for a short time period after treatment initiation.

Under these assumptions, we find that the mutant virus,  $V_2(t)$ , after therapy is initiated is determined by a sum of several exponentials, and is dominated by a term of the form  $e^{\theta_2 t}$ , where  $\theta_2 = \left[ -(c_2 + \delta_2) + \sqrt{(c_2 - \delta_2)^2 + 4k_2 N_2 (1 - e_2) \delta_2 T(0)} \right] / 2$ . The pre-treatment quasi-steady-state analysis leading to (3) places constraints on the parameter values, which imply that  $\theta_2$  is negative. Thus, the mutant virus decreases initially. We only expect this dynamic analysis to be valid for a short period of time, since we have assumed  $T(t) = T(0)$ . However, because the viral load changes much faster and more dramatically than the CD4<sup>+</sup> T cell concentration [5, 6], a reasonable approximation for the dynamics of  $V_2(t)$  over longer time periods can be constructed by replacing the pre-treatment value  $T(0)$  by the dynamic value  $T(t)$  in the expression for  $\theta_2$ . That is, we claim that a good approximation for the mutant viral load is

$$V_2(t) = V_2(0) - C + C e^{\int_0^t \theta_2(s) ds}, \quad \text{where } \theta_2(t) = \frac{-(c_2 + \delta_2) + \sqrt{(c_2 - \delta_2)^2 + 4k_2 N_2 (1 - e_2) \delta_2 T(t)}}{2}. \quad (5)$$

Numerical solutions of the model (equations (14)-(16), (20)-(23) in the Appendix) using the data in Table 1 and Figure 4 confirm that this approximation is accurate: When the proportionality constant  $C$  is chosen appropriately, the absolute value of the relative error of our approximation for  $\log_{10} V_2(t)$  averaged over the first 500 days (i.e.,  $\int_0^{500} (|\log_{10} V_2(t) - \log_{10} \{V_2(0) - C + C e^{\int_0^t \theta_2(s) ds}\}| / V_2(t)) dt / 500$ ) is 1.0%, and the trajectory of  $\log_{10} V_2(t)$  is visually indistinguishable from its approximation. However, the accuracy of (5) deteriorates in the full model that includes long-lived cells because it fails to capture the second phase of the biphasic viral decay curve.



Equation (5) implies that after therapy is initiated the mutant virus  $V_2(t)$  will drop. However, if  $\theta_2(t)$  changes sign and becomes positive, then  $V_2(t)$  declines to a nadir and begins to increase when  $\theta_2(t)$  first becomes positive. Assuming the clearance rate constants of the mutant and wild-type virus are equal, this occurs when  $T(t)$  (respectively,  $CD4^+(t)$ ) rises to the level

$$\frac{T(0)}{\eta f(1 - e_2)} = \frac{1.05T(0)}{1 - e_2} \quad (\text{respectively, } \frac{CD4^+(0)}{1 - e_2}), \quad (6)$$

where again as an illustration we have chosen  $\eta = 0.96$  and  $CD4^+(0) = 1.05 T(0)$ . Similarly,  $V_2(t)$  will reach a peak and then begin to decrease again when and if  $\theta_2(t)$  becomes negative again. The oscillations in viral load (and T cell count) are what have been called predator-prey oscillations. As the viral load decreases, the T cell count recovers. This provides additional targets for viral infection, and if the antiretroviral therapy is not sufficiently active against mutant virus, the virus can replicate. Whether the virus will replicate depends both on the efficacy of the drug regime and the T cell count as indicated by equation (6).

The hypothesized reversal in the viral load decline as the  $CD4^+$  T cell count increases is confirmed by Figure 4, which displays the exact numerical solutions to the full model for a particular example. Although equation (5) is not an accurate approximation in the full ten-dimensional model that includes long-lived cells, Figure 4 shows that the concomitant  $CD4^+$  crossing times and viral extremes predicted in (6) do indeed hold for the full ten-dimensional model. We also computed numerical solutions of the full model under various values of the  $CD4^+$  proliferation rate  $\lambda$ , the maximum uninfected  $CD4^+$  count  $T_{\max}$  and the drug efficacy against the mutant virus,  $e_2$ , because these parameters vary significantly across HIV-1-infected individuals. When  $\lambda$  is increased from  $0.01 \text{ day}^{-1}$  to  $0.068 \text{ day}^{-1}$  (the value suggested by Figure 2b of [6]), the  $CD4^+$  count rises to almost  $T_{\max}$  within several months and the mutant virus emerges much earlier. There are also less pronounced oscillations, and the system attains a new steady state within eight months. An increase in  $T_{\max}$  from 450 to

680 (Figure 2b of [6]) also induces an effective increase in the T cell proliferation rate, which speeds up the dynamics of the system. Finally, smaller values of  $e_2$  lead to earlier emergence of the mutant strain.

### Maintenance Therapy

One possible strategy under consideration for management of HIV-infected patients is to administer a potent antiretroviral regime to rapidly bring the viral load to an undetectable level and then to reduce the potency of the drug regime by withdrawing one or more of the drugs. This would decrease the drug cost and diminish the risk of drug toxicity and other possible long-term side-effects. Here we analyze the potential consequences of such a treatment strategy within our model.

Assume a powerful inductive regimen is applied at time zero and that at time  $t_m$ , the patient is switched to a less intensive maintenance therapy. Because a switch to maintenance therapy would only be recommended if virus suppression is maintained, we assume in our mathematical analysis that resistant virus has not arisen and, because of the low viral load, will not arise during maintenance therapy. Thus we omit the mutant virus strain from the analysis, i.e., we assume that  $T_2^* = M_2^* = V_2^I = V_2 = m_{12} = m_{21} = 0$ , thereby reducing our original model from ten equations to six. However, we also use numerical methods to analyze the case in which resistant virus does arise during induction therapy but remains below the detection limit. In this case, during maintenance therapy the resistant strain can either grow or be eradicated.

In this section, the system is only analyzed from time  $t_m$  onwards. The mathematical analysis of the steady-state and dynamic behavior of the model is essentially equivalent to our earlier analysis, and so we omit the analysis and only present the main results.

**Steady-state results.** The key question in this setting is: Under what conditions

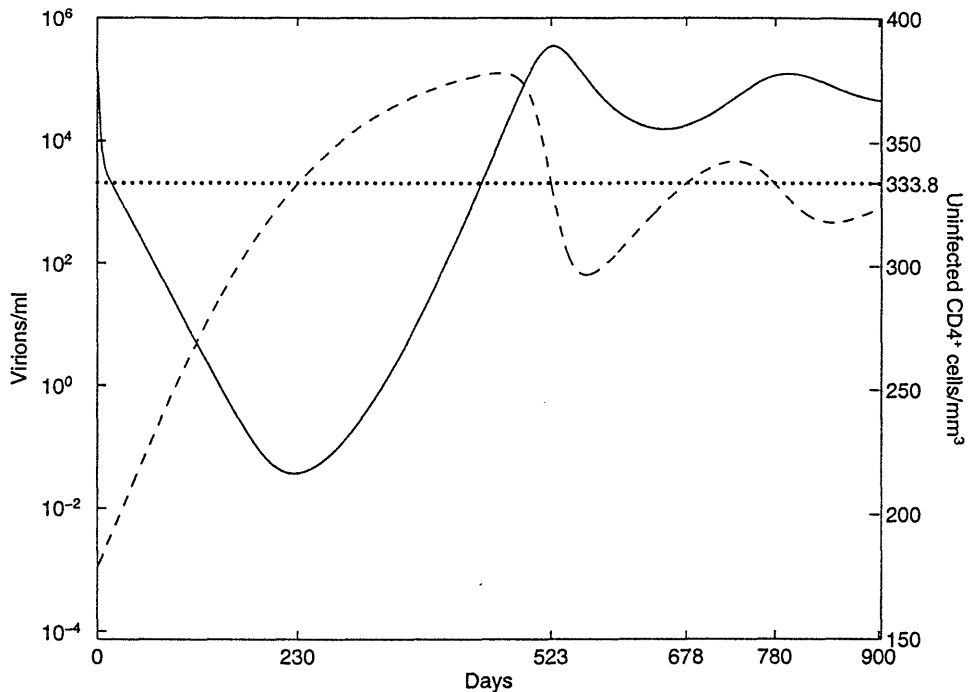


Figure 4: The dynamics of the total virus,  $V(t)$  (solid line), and the uninfected  $CD4^+$  T cells,  $T(t)$  (dashed line), in a case where mutant virus breaks through combination therapy as computed from the full ten-equation model given in the Appendix. The efficacy of the combination therapy is  $r_1 = 0.9$ ,  $p_1 = 0.99$ ,  $r_2 = p_2 = 0.25$ . The wild-type viral load,  $V_1(t)$ , follows a biphasic curve and drops below 0.25 (which corresponds to the detection limit of the standard branched DNA assay of 500 HIV-1 RNA copies/ml) on day 50. Although the virus is no longer detectable, the theory predicts that  $V_1$  continues to decay so that the rebound in total viral load seen after day 230 is due to the growth of mutant virus. We predict that the mutant viral load attains a peak (respectively, nadir) at about the time when the infected  $CD4^+$  cell concentration passes through the value given by equation (6), which for the parameters in Table 1 equals 333.8 (dotted line) from below (respectively, above). We have also assumed  $\eta = 0.96$  and  $f = 0.99$ . The  $CD4^+$  crossing times, days 230, 523, 678 and 780, coincide well with the corresponding times for the viral extremes, days 225, 526, 653 and 795, respectively. After several of these oscillations, the mutant viral load and the uninfected  $CD4^+$  count settle into steady-state levels that are close to the values  $V_2 = 6.91 \times 10^4$  virions/ml,  $T = 326.9$  cells/mm<sup>3</sup> calculated in the Appendix.

will the maintenance regimen eradicate the wild-type virus? The answer is if

$$e_1 > 1 - \frac{\lambda c_1}{(\lambda - \mu)k_1 N_1 T_{\max}}, \quad (7)$$

or for a patient in quasi-steady state before therapy was begun, so that  $N_1 k_1 T(0) = \eta c_1$ , if

$$e_1 > 1 - \frac{1}{\eta} \left( \frac{\lambda}{\lambda - \mu} \right) \frac{T(0)}{T_{\max}}. \quad (8)$$

These are in essence equations (3) and (4) for the wild-type virus. If we assume  $\eta = 0.96$ ,  $\lambda = 1.16(\lambda - \mu)$  and that 5% of CD4<sup>+</sup> T cells are infected at treatment initiation, then the condition reduces to

$$e_1 > e_{1c} \equiv 1 - 1.15 \frac{CD4^+(0)}{CD4^+_{\max}}. \quad (9)$$

Using equation (8), we compute in Table 3 the critical maintenance drug efficacy,  $e_{1c}$ , required to completely eradicate the virus for various values of  $T(0)$  and  $T_{\max}$ . Notice that if the initial T cell count is high, the drug regime need not be very efficacious (recall  $e = 1$  implies a completely inhibitory regime).

The steady-state viral load and CD4<sup>+</sup> T cell count as a function of the strength of the maintenance therapy are well described by Figure 3, with the subscript 1 in place of the subscript 2. The intersection of these two curves with the vertical axis corresponds to the pre-treatment quasi-steady-state values. Hence, the model predicts that it is difficult to find a maintenance therapy to maintain viral loads at a low level; a maintenance therapy is highly likely to either eradicate the virus or allow the viral load to return to near its pre-treatment value.

$T(0)$	$T_{\max}$	$e_{1c}$
50	200	0.698
50	400	0.849
50	600	0.899
50	800	0.924
50	1000	0.936
100	200	0.396
100	400	0.698
100	600	0.799
100	800	0.849
100	1000	0.879
200	400	0.396
200	600	0.597
200	800	0.698
200	1000	0.758
400	600	0.194
400	800	0.396
400	1000	0.517
600	800	0.094
600	1000	0.275
800	1000	0.033

Table 3: The critical maintenance drug efficacy,  $e_{1c}$ , for various values of  $T(0)$  and  $T_{\max}$ , where  $\eta = 0.96$  [3] and  $\lambda = 1.16(\lambda - \mu)$ .

**Dynamic results.** The goal here is to analyze the dynamic behavior of the system after the switch to a maintenance therapy. As in the previous dynamic analysis, we omit the long-lived cell terms, and hence only analyze a system of four equations: (14), (15), (20) and (22) in the Appendix. By our earlier analysis, the viral load  $V_1(t)$  after time  $t_m$  is approximated by  $V_1(t_m) - C + Ce^{\int_{t_m}^t \theta_1(s) ds}$ , where  $\theta_1(t)$  is defined similarly to  $\theta_2(t)$  (5), but with the subscript 2 replaced by the subscript 1. Hence, we predict that immediately after the switch in therapy, the viral load decreases exponentially if  $\theta_1(t_m)$  is negative, i.e, if

$$e_1 > 1 - \frac{1}{\eta} \frac{T(0)}{T(t_m)} = 0.99 \frac{CD4^+(0)}{CD4^+(t_m)}, \quad (10)$$

where the equality sign is based on our example values of  $\eta = 0.96$  and  $CD4^+(0)=1.05 T(0)$ . There are three cases that are likely to occur (the mathematical existence of the fourth case may be due to the different assumptions used in the steady-state and dynamic analyses): If the maintenance therapy is very strong (i.e., if equations (8) and (10) are satisfied) then the viral load initially decreases and eventually is eradicated. If the maintenance therapy is intermediate in strength (i.e., if (8) is violated and (10) is satisfied) then the viral load initially decreases but eventually attains a positive steady state; we have only observed this case numerically when the switch to a maintenance therapy is very early, so that  $T(t_m)$  is much smaller than  $T_{\max}$ . Finally, if the maintenance therapy is relatively weak (i.e., both (8) and (10) are violated) then the virus initially increases exponentially, attains a peak (respectively, trough) when the uninfected  $CD4^+$  count  $T(t)$  reaches the level

$$\frac{1}{\eta} \frac{T(0)}{1 - e_1} \tag{11}$$

from above (respectively, below), and slowly settles into a positive steady state. The dynamics for this last case are illustrated in Figure 5, which shows the exact numerical solution of the six-equation model that includes long-lived cells but omits mutant virus.

Figure 6 compares a weak maintenance therapy versus discontinuation of therapy at nine months. Relative to maintenance therapy, discontinuation of therapy leads to a much steeper viral increase, a higher initial viral peak, more pronounced oscillations and a slightly higher steady-state viral load. In fact, the model predicts that the viral load returns to its pre-treatment level after discontinuation, which is consistent with anecdotal evidence of discontinuation [25, 26]. Because discontinuation leads to a very rapid increase in the viral load, it should become apparent in a matter of weeks after therapy is stopped if the virus has been eradicated. In this example, without the switch to maintenance therapy, the virus

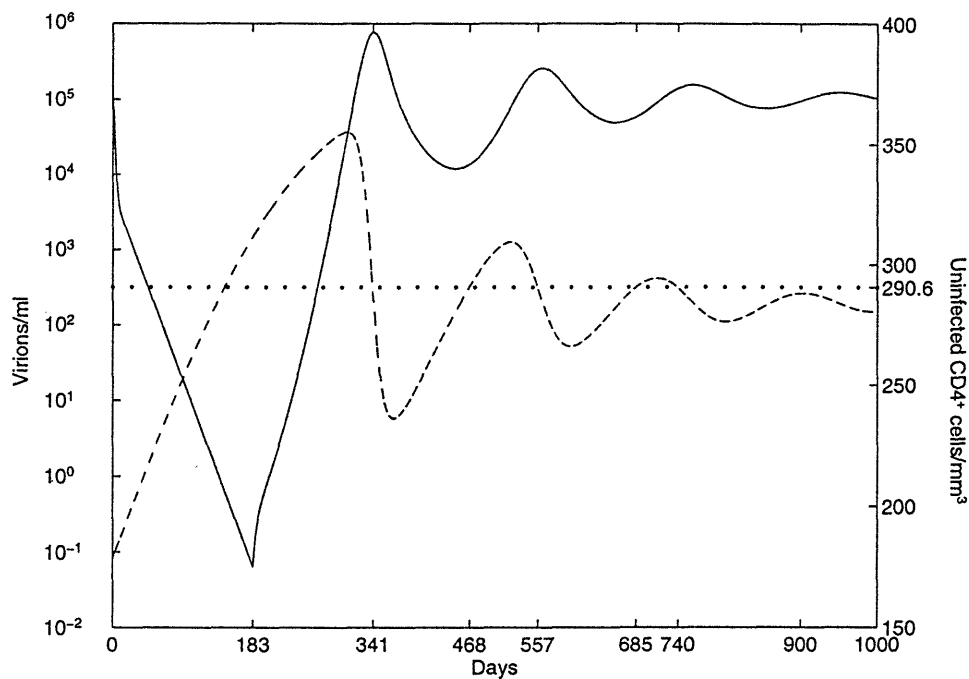


Figure 5: The dynamics of the viral load,  $V_1(t)$  (solid line), and the uninfected  $CD4^+$  T cell count,  $T(t)$  (dashed line), before and after maintenance therapy computed from the model without mutant virus. The combination therapy  $r_1 = 0.9$ ,  $p_1 = 0.99$  is applied from time zero until time  $t_m = 6$  months. At time  $t_m$ , the patient is switched to a low efficacy maintenance therapy given by  $r_1 = p_1 = 0.2$ . As predicted, the virus initially rises after time  $t_m$  and achieves its maximum on day 342, which coincides well with the time (day 341) at which  $T(t)$  drops to the critical level of 290.6 (dotted line) predicted by equation (11). The subsequent times of viral extremes are days 450, 563, 658 and 760, compared to the corresponding uninfected  $CD4^+$  crossing times of days 468, 557, 685 and 740. The oscillations eventually dissipate and the viral load and uninfected  $CD4^+$  count stabilize near the steady-state levels  $V_1 = 104.7 \times 10^3$  virions/ml,  $T = 283.5$  cells/mm<sup>3</sup> predicted in the Appendix.

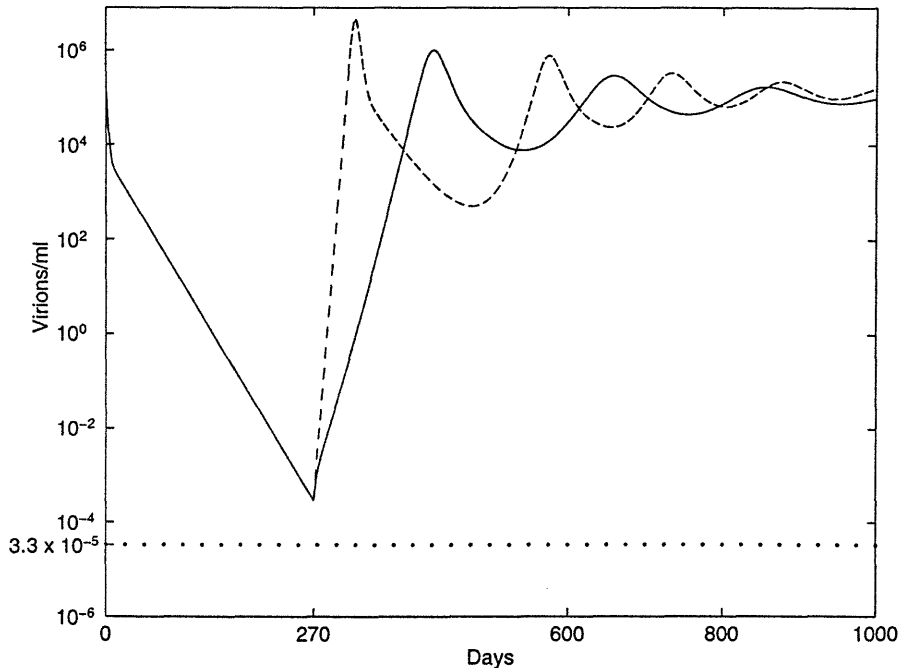


Figure 6: The dynamics of the viral load  $V_1(t)$  when induction therapy ( $r_1 = 0.9, p_1 = 0.99$ ) is switched to maintenance therapy ( $r_1 = p_1 = 0.2$ ) at nine months (solid line) or is discontinued at nine months (dashed line). Without a switch to maintenance therapy, the virus would be eradicated, which corresponds in the model to dropping below the level of one virion in the extracellular fluid compartment of the body (dotted line), on day 305 and would stay eradicated (not shown).

would have been eradicated on day 305. Here the criterion for eradication is having the virion concentration fall below one virion in 15 liters, the extracellular fluid volume in a typical adult. A more stringent criterion would delay eradication somewhat.

The basic qualitative results in Figures 5 and 6 also hold for higher values of the  $CD4^+$  proliferation rate  $\lambda$  and the maximum uninfected  $CD4^+$  value,  $T_{\max}$ . Higher values of  $\lambda$  and lower values of  $T_{\max}$  allow the  $CD4^+$  cell count to nearly attain the value of  $T_{\max}$  at the time of discontinuation. Consequently, in these cases the post-maintenance oscillations are less pronounced and dissipate quicker than in Figures 5 and 6.

Our formal mathematical model for maintenance therapy assumes that no mutant virus is present. More realistic numerical calculations are shown in Figure 7 and Table 4. Here we



have simulated the ten-equation model under the proposed protocol of ACTG 343 [4] in which patients on combination therapy will either continue receiving RT and protease inhibitors, or at six months have either the protease inhibitor indinavir or the RT inhibitors ZDV and 3TC discontinued. As we have tried to emphasize throughout, the precise outcome will depend heavily on the efficacy of the drug regime against the mutant virus. This dependence can be seen in Table 4, which displays the outcome (either the day the virus becomes detectable or the day the virus is eradicated) under the three arms of ACTG 343 for various values of the maintenance drug efficacy against the mutant virus,  $(r_2, p_2)$ , and the relative fitness of the mutant,  $f$ . When  $r_2 = p_2 = 0.55$  in Table 4, eradication is achieved under both maintenance arms; in contrast, under the more pessimistic values of  $r_2 = 0.2$ ,  $p_2 = 0.4$  in Table 4, neither maintenance arm is able to eradicate the virus. Our model predicts that the two maintenance arms will achieve the same outcome as when they are used for induction therapy; hence, we predict that the ZDV-3TC arm will not be able to eradicate the virus but will achieve about a one log reduction from the pretreatment steady-state viral load [24], and that indinavir monotherapy will maintain the viral load below the level of detection for one year in only a minority of patients [27, 28]. To be conservative we have assumed that the mutant virus has a high relative fitness. However, as can be seen in the first two blocks of the table, assuming a lower relative fitness only makes a small change in the time of detection.

	$r_2$	$p_2$	$f$	Therapy	Day of Detection	Day of Eradication
1	0.25	0.25	0.99	RT	236	–
2	0.25	0.25	0.65	RT	270	–
3	0.25	0.25	0.99	Protease	236	–
4	0.25	0.25	0.99	Both	413	–
5	0.35	0.35	0.99	RT	301	–
6	0.35	0.35	0.75	RT	330	–
7	0.35	0.35	0.99	Protease	301	–
8	0.35	0.35	0.99	Both	–	307
9	0.45	0.45	0.99	RT	498	–
10	0.45	0.45	0.99	Protease	498	–
11	0.45	0.45	0.99	Both	–	306
12	0.55	0.55	0.99	RT	–	312
13	0.55	0.55	0.99	Protease	–	308
14	0.55	0.55	0.99	Both	–	306
15	0.2	0.4	0.99	RT	236	–
16	0.2	0.4	0.99	Protease	354	–
17	0.2	0.4	0.99	Both	–	330
18	0.3	0.5	0.99	RT	273	–
19	0.3	0.5	0.99	Protease	1112	–
20	0.3	0.5	0.99	Both	–	306
21	0.4	0.6	0.99	RT	366	–
22	0.4	0.6	0.99	Protease	–	306
23	0.4	0.6	0.99	Both	–	305

Table 4: Simulation of the three arms of the proposed ACTG 343 study for various values of the mutant drug efficacy,  $(r_2, p_2)$ , and the relative fitness of the mutant virus,  $f$ . At six months, the induction therapy ( $r_1 = 0.9$ ,  $p_1 = 0.99$  and  $r_2, p_2$  above) is switched to a maintenance therapy of only RT inhibitors (RT) or only the protease inhibitor (Protease), or is continued (Both). In all 23 scenarios, either the virus becomes detectable again (i.e., attains the level of 500 HIV-1 RNA copies/ml) or is completely eradicated (i.e. drops below one virion in the extracellular fluid volume of the body). The viral dynamics of scenarios 15-17 are graphed in Figure 7.

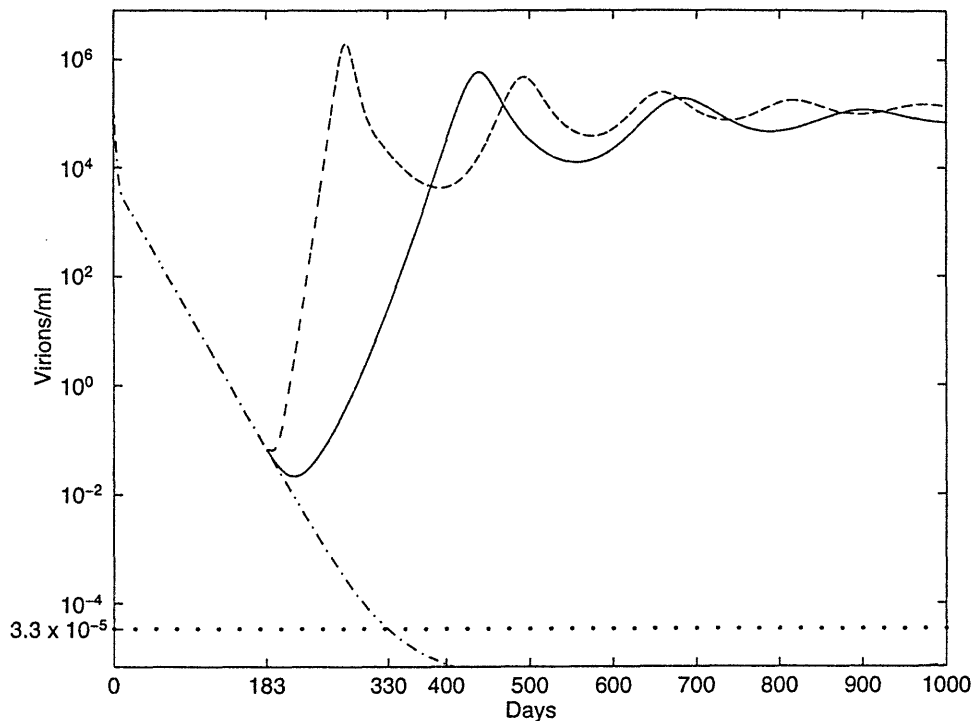


Figure 7: Simulation of the three arms of the ACTG 343 study. The viral load  $V(t)$  is computed from the full model assuming induction therapy ( $r_1 = 0.9$ ,  $p_1 = 0.99$ ,  $r_2 = 0.2$ ,  $p_2 = 0.4$ ; see Table 4 for less pessimistic values for  $r_2$  and  $p_2$ ) is either continued (dashed-dotted line), or switched at six months to maintenance therapy using only RT inhibitors, i.e.,  $r_1 = 0.9$ ,  $r_2 = 0.2$ ,  $p_1 = p_2 = 0$  (dashed line) or only protease inhibitors, i.e.  $p_1 = 0.9$ ,  $p_2 = 0.4$ ,  $r_1 = r_2 = 0$  (solid line). In this example, continuation of the combination therapy is predicted to lead to eradication at day 330 when the viral load passes a threshold value (dotted line), here corresponding to one virion in the total extracellular fluid of the body. The two maintenance therapies are predicted to result in emergence of the mutant virus. Note, if the maintenance therapy were delayed to one year while keeping the other parameter values fixed as above, then the model would predict eradication.

## Discussion

Our mathematical analysis yields very simple conditions for the eradication of the virus. The eradication condition is given by (7) in the absence of mutant virus and by (2) in the presence of mutant virus. If the mutant virus is nearly as fit as the wild-type virus then these conditions are almost identical. Also, the eradication condition for maintenance therapy is the same as the eradication condition for induction therapy, despite the fact that induction therapy is apt to be faced with a higher initial viral load. More generally, the analysis predicts that the performance of a maintenance therapy will be similar to its performance as an induction therapy, unless the virus unknowingly has already been totally eradicated at the time of the switch to maintenance therapy. Consequently, if induction therapy is unable to eradicate the virus then the outcome (e.g. new steady-state viral load and CD4<sup>+</sup> count) of maintenance therapy is *independent* of the timing of the switch to maintenance therapy. These results suggest that a drug combination that is very effective against the wild-type virus but only moderately effective against the mutant virus will only achieve transient suppression and will not eradicate the virus; for eradication to occur, the antiviral regimen must be nearly as effective against the mutant strains as against the wild-type strain. Hence, research efforts should focus on constructing drug combinations that are sufficiently (in the sense of equations 2 and 7) efficacious against all strains that may pre-exist or arise during the course of therapy (see also [29]).

The eradication conditions are not relevant if the drug efficacy against the wild-type is 100% ( $r_1 = p_1 = 1$ ) and there is no mutant virus initially ( $V_2(0) = T_2^*(0) = M_2^*(0) = 0$ ). In this case it is not possible to produce mutant virus and eradication is certain to occur. This scenario is not likely to arise in clinical practice because a variety of partially drug-resistant strains are usually present at low levels (near 1%) in drug-naive individuals [30].

The model on which our predictions are based is deterministic. A probabilistic model

would more realistically capture the mutation-selection process and the viral dynamics when the viral load becomes low somewhere along its trajectory. Extrapolating from results for simpler models [31], we expect that in a properly formulated stochastic model the eradication conditions would take on a probabilistic flavor, e.g., if (2) or (7) hold then a large steady-state viral load is highly unlikely; if these conditions are violated then there is still a (perhaps small) chance that the virus will be eradicated.

The pre-treatment quasi-steady-state assumption allows us to express the eradication conditions (2) and (7) in a more transparent form; see equations (3)-(4) and (8)-(9). These inequalities highlight the fact that eradication is essentially determined by two factors: the drug efficacy  $e_i$  and the ratio  $T(0)/T_{\max}$  of the pre-treatment uninfected CD4<sup>+</sup> cell concentration divided by the maximum achievable concentration. Preliminary estimates of the ratio  $T(0)/T_{\max}$  suggest that the drug efficacy required for eradication of a strain of virus is in the 0.6 to 0.9 range, which should be satisfied by most drug combinations against a wild-type virus, but may not be satisfied against drug-resistant strains.

The ratio  $T(0)/T_{\max}$  arises as a result of *predator-prey* (or host-parasite) dynamics: The smaller this ratio, the larger the potential relative increase in the pool of uninfected CD4<sup>+</sup> T cells (prey), and the more difficult it is to eventually eradicate the virus (predator). Predator-prey effects have been observed in many mathematical models for HIV [8, 9, 10, 11, 12, 32] and have recently been used to offer a possible explanation for the reduction in virus during primary infection [33] and to explain the initial loss of viral suppression under AZT therapy [13, 14]. To the extent that  $T_{\max}$  corresponds to the potential capacity of a person's immune system, our results suggest the perhaps counterintuitive notion that individuals with potentially stronger immune systems (as measured by their potential for CD4<sup>+</sup> T cell recovery) require more powerful drug regimens for eradication. These results also imply that it is easier to eradicate the virus when the pre-treatment CD4<sup>+</sup> count,  $T(0)$ ,

is high (this increases the ratio  $T(0)/T_{\max}$ ), which is consistent with the “hit early, hit hard” philosophy [34]; Table 3 articulates this philosophy in quantitative terms. Also, the eradication conditions depend on the viral burst sizes  $N_i$  and  $N_i^M$ , the smaller the burst sizes the easier it is to eradicate (see equation 27). Because a CTL response may kill the cells before much viral release occurs, which would effectively reduce the burst sizes  $N_i$  and  $N_i^M$ , the stronger the CTL response the easier it is to eradicate the virus.

The steady-state results in the Appendix and Figure 3 offer more refined information than the eradication condition, by predicting the new steady-state viral load if eradication does not occur. The steep drop of the viral load curve in Figure 3 suggests that after induction or maintenance therapy, the virus is likely to either be eradicated or return to roughly its pre-treatment level. Table 2 provides a range of drug efficacies against the mutant virus and relative fitness of the mutant virus that will result in a non-zero viral load that is significantly less than the pre-treatment viral load.

Our dynamic analysis reinforces the notion that the predator-prey dynamics between the uninfected pool of cells and the virus is a driving factor behind system behavior. In particular, equation (5) allows us to predict the viral dynamics in terms of the *trajectory* of the  $CD4^+$  count; previous models (e.g., [3, 5, 6, 7]) predict the viral dynamics only in terms of the *initial*  $CD4^+$  count, and so are only valid for short time intervals. Numerical solutions confirm the accuracy of (5) and two of its implications: The mutant virus emerges at about the time when the uninfected pool of  $CD4^+$  cells  $T(t)$  first rises to the level in equation (6), and the viral load after the switch to maintenance therapy has a peak (nadir, respectively) when  $T(t)$  crosses the level in equation (11) from above (below, respectively). The first implication predicts a positive correlation between the observed increase in  $CD4^+$  cell count during therapy and the speed or likelihood of mutant viral escape. This prediction is consistent with Figures 1 and 5 in [35], where low-dose saquinavir leads to a higher

and faster initial CD4<sup>+</sup> increase and a quicker emergence of mutant virus than high-dose saquinavir. Nonetheless, it remains to rigorously test equation (5) using clinical data.

Equation (5) can also be used to estimate the slope of the initial viral drop after the administration of an imperfect drug regimen. If we assume that the patient has very little mutant virus and is in quasi-steady state before therapy, then after therapy is initiated, the wild-type viral load,  $V_1(t)$ , decays exponentially at rate  $\theta_1$ , where

$$\theta_1 = \frac{-(c_1 + \delta_1) + \sqrt{(c_1 - \delta_1)^2 + 4\eta(1 - e_1)\delta_1}}{2}. \quad (12)$$

For the typical values of  $c_1 = 3.07$  [7],  $\delta_1 = 0.69$  [3] and  $\eta = 1.0$  (the initial viral drop occurs during the first phase of the biphasic curve in [3], before long-lived cells have a major effect), numerical plots of  $\theta_1$  as a function of the drug efficacy,  $e_1$ , reveal that  $\theta_1$  is well approximated by  $-e_1\delta_1$ . Hence, the predicted rate of viral decay for a drug combination of efficacy  $e_1$  is simply  $e_1\delta_1$ . Note that a completely ineffective regimen,  $e_1 = 0$ , causes no reduction in the viral load,  $\theta_1 = 0$ , and a completely effective regime,  $e_1 = 1$ , gives the results in [6, 5],  $\theta_1 = -\delta_1$ . (When  $e_1 = 1$  another solution to equation 12 is  $\theta_1 = c_1$ . This is the rate at which virions would be cleared if there were no productively infected cells present).

Although our dynamic analysis of (14)-(23) shows that the transient behavior is dictated primarily by the drug efficacy and the predator-prey dynamics, other factors still play a significant, albeit smaller, role. In particular, the mutant viral load,  $V_2(t)$ , increases linearly with the initial mutant viral load  $V_2(0)$  and the mutation probability  $m_{12}$ , and decreases linearly with the efficacy of the RT inhibitors against the wild-type virus,  $r_1$ . Equations (33)-(34) in the Appendix quantify the relative importance of pre-existing mutant virus, ( $T_2^*(0)$ ,  $V_2(0)$ ), versus mutant virus that is generated during therapy due to escape from the RT inhibitor (determined by  $m_{12}$ ,  $r_1$ , and  $V_1(0)$ ). Equations (36) and (38) in the Appendix imply that the pre-existing mutant virus is the more dominant of these two factors if either the

pre-treatment fraction of virus that is mutant is significantly larger than  $3.6 \times 10^{-5}$  or if the concentration of  $CD4^+$  cells infected by mutant virus at the start of therapy,  $T_2^*(0)$ , is significantly larger than  $5 \times 10^{-4}$  cells/mm<sup>3</sup>. These calculations, as well as the findings in [30, 36], suggest that pre-existing mutant virus is the more dominant factor in most HIV-1-infected individuals. This conclusion is consistent with recent evidence that new strains do not seem to arise under potent therapeutic regimens [28].

Implicit in model (14)-(23) are three very important assumptions. First, we consider only two compartments of cells,  $CD4^+$  T cells, which when productively infected are short-lived, and a longer-lived productively infected cell compartment. We thus ignore the possible existence of any even slower decaying, small compartments or any sanctuaries (e.g., the brain or the central nervous system [39]) that are unaffected by the antiretroviral agents. Second, our model only contains one mutant HIV-1 strain. If new strains do not arise under potent therapeutic regimens (cf. [28]), then the mutant strain in our model can be interpreted as a surrogate for the pre-existing strain that is most likely to emerge under the modeled combination therapy. Such a strain typically would have a high level of drug resistance (i.e., a low value of  $e_2$ , the drug efficacy), and a high fitness,  $f$ . If therapy was sufficiently potent to eradicate the surrogate strain, we would expect all strains to be eradicated; hence, for purposes of steady-state analysis, it suffices to include only one mutant strain in our model, as long as it is interpreted appropriately. Because significant phenotypic resistance requires the stepwise accumulation of multiple mutations in HIV-1 protease [37], the drug efficacy against the mutant virus,  $e_2$ , (and hence the likelihood of eradication) is likely to depend greatly on the specific viral strains that exist prior to treatment: patients who possess pre-existing multiple mutations would be expected to have lower  $e_2$  values (i.e. greater phenotypic drug resistance) than patients that have only single mutations. To the extent that patients in more advanced disease stages are more apt to have lower values of  $e_2$ , equation (3) predicts



that viral eradication would be more difficult to achieve in these patients, as observed in [38].

Finally, we also assume that the immune system remains constant over the time period of study. While this assumption might be reasonable for short periods of time, there is reason to believe that some of the model's parameters might change if the virus and CD4<sup>+</sup> count experience major fluctuations. In particular, the parameter  $T_{\max}$ , which is indicative of the recuperative powers of the immune system, might increase when the virus is suppressed to very low levels [40]. Also, the loss rates of infected cells,  $\delta_i$  and  $\delta_i^M$ , may change. The loss rates may increase over the course of combination therapy because of restored immune function and an increase in memory cells; on the other hand, the decrease in infected cells during combination therapy may lead to diminished stimulation of a CTL response, and a reduction in the loss rates.

To investigate the assumption regarding a constant immune system, we re-solved the discontinuation case in Figure 6, but assumed that the parameters  $T_{\max}$ ,  $\delta_1$  and  $\delta_1^M$  vary over time according to

$$T_{\max}(t) = T_{\max} a^{T(t)-T(0)}, \quad \delta_1(t) = \delta_1 a^{T(t)-T(0)} \quad \text{and} \quad \delta_1^M(t) = \delta_1^M a^{T(t)-T(0)}, \quad (13)$$

where the constant  $a$  was chosen so that  $a^{100} = 1 + \epsilon$ ; that is, every increase in the uninfected CD4<sup>+</sup> T cell count of 100 causes an  $\epsilon \times 100\%$  increase in these parameter values. However, we kept the viral production rates per unit time,  $\pi_i = N_i \delta_i$  and  $\pi_i^M = N_i^M \delta_i^M$  in equations (20)-(23), constant at their original values. First, allowing only  $T_{\max}$  to change by setting  $\epsilon = 0.05$  and 0.1 for  $T_{\max}$  only, we found that the viral spike after maintenance therapy and the subsequent steady-state viral load were higher with larger values of  $\epsilon$ , and the steady-state CD4<sup>+</sup> count was not significantly affected by changes in  $\epsilon$ . Dynamically increasing the value of  $T_{\max}$  during induction therapy forces further increases in the CD4<sup>+</sup> count after discontinuation, which exacerbates the predator-prey dynamics and makes eradication more

difficult. In contrast, larger values of  $\epsilon$  for the cell loss rates  $\delta_i$  and  $\delta_i^M$  led to a decrease in the viral spike and steady-state viral loads, and an increase in the steady-state CD4<sup>+</sup> count. Hence, if the infected cell loss rates are significantly increased during induction therapy, as in (13), then the eradication condition for maintenance therapy is less stringent than under induction therapy. When  $\epsilon$  is set equal to 0.05 for all three parameters in (13) simultaneously, the effect of  $T_{\max}$  appears to win out, and there is an increase in the viral peak and steady-state viral load.

### Acknowledgment

We thank Brad Saget and Steve Scheibel for useful conversations and for sharing some of their data, and Diane V. Havlir, Douglas D. Richman, Nikolas Stilianakis, Paulina Essunger and John Mittler for comments on an earlier version of the manuscript. Discussions with Avidan Neumann and Elissa Schwartz on a simpler model containing drug efficacy effects were also helpful. Portions of this work were performed under the auspices of the U.S. Department of Energy. A.S.P. acknowledges support from NIH grant RR06555 and the Santa Fe Institute through a grant from the Jeanne M. Sullivan and Joseph P. Sullivan Foundation. L.M.W. was supported by National Science Foundation grant DDM-9057297 and R.M.D. was supported by a National Defense Science and Engineering Graduate Fellowship from the Department of Defense.

## References

- [1] Gulick RM, Mellors J, Havlir D, Eron J *et al.*: Potent and sustained antiretroviral activity of indinavir (IDV), zidovudine (ZDV) and lamivudine (3TC). *XI International Conference on AIDS*, Vancouver, July 11 1996, Abstr. Th.B.931.
- [2] Markowitz, M., Cao, Y, Hurley A, O'Donovan, R *et al.*: Triple therapy with AZT, 3TC, and ritonavir in 12 subjects newly infected with HIV-1. *XI International Conference on AIDS*, Vancouver, July 11 1996, Abstr. Th.B.933.
- [3] Perelson AS, Essunger P, Cao Y, Vesanen M, Hurley A, Markowitz M, Ho DD: Decay characteristics of long-lived HIV-1-infected compartments: A minimal estimate of the treatment time needed for eradication of the virus (submitted).
- [4] Havlir DV, Richman DD (Protocol Chairs): ACTG 343: A prospective randomized double blind trial of three maintenance regimens for HIV infected subjects receiving induction therapy with zidovudine, lamivudine and indinavir (draft). 1996.
- [5] Wei X, Ghosh SK, Taylor ME, Johnson VA *et al.*: Viral dynamics in human immunodeficiency virus type 1 infection. *Nature* 1995, 373:117-123.
- [6] Ho DD, Neumann AU, Perelson AS, Chen W, Leonard JM, Markowitz M: Rapid turnover of plasma virions and CD4 lymphocytes in HIV-1 infection. *Nature* 1995, 373:123-126.
- [7] Perelson AS, Neumann AU, Markowitz M, Leonard JM, Ho DD: HIV-1 dynamics in vivo: virion clearance rate, infected cell lifespan, and viral generation time. *Science* 1996, 271:1582-1586.

- [8] McLean AR, Emery VC, Webster, A, Griffiths PD: Population dynamics of HIV within an individual after treatment with zidovudine. *AIDS* 1991, 5:485-489.
- [9] McLean AR, Nowak MA: Competition between zidovudine sensitive and resistant strains of HIV. *AIDS* 1992, 6:71-79.
- [10] Frost SDW, McLean AR: Quasispecies dynamics and the emergence of drug resistance during zidovudine therapy of HIV infection. *AIDS* 1994, 8:323-332.
- [11] McLean AR, Frost SDW: Zidovudine and HIV: Mathematical models of within-host population dynamics. *Rev. Med. Virol.* 1995, 5:141-147.
- [12] de Boer RJ, Boucher CAB: Anti-CD4 therapy for AIDS suggested by mathematical models. *Proc. Roy. Soc. London B* 1996, 263:899-903.
- [13] de Jong MD, Veenstra J, Stilianakis NI, Schuurman R, Lange JMA, de Boer RJ, Boucher CAB: Host-parasite dynamics and outgrowth of virus containing a single K70R amino acid change in reverse transcriptase are responsible for the loss of HIV-1 RNA load suppression by zidovudine. *Proc. Natl. Acad. Sci. USA* 1996, 93:5501-5506.
- [14] Stilianakis NI, Boucher CAB, de Jong MD, van Leeuwen R, Schuurman R, de Boer RJ: Clinical data sets on human immunodeficiency virus type 1 reverse transcriptase resistant mutants explained by a mathematical model. *J. Virol.* 1997, 71:161-168.
- [15] Nowak MA, Bonhoeffer S, Shaw GM, May RM: Anti-viral drug treatment: dynamics of resistance in free virus and infected cell population. *J. Theoret. Biol.* 1997, 184:203-217..
- [16] Wein LM, Zenios S, Nowak MA: Dynamic multidrug therapies for HIV: A control theoretic approach. *J. Theoret. Biol.* (in press)

- [17] Nowak MA, Bonhoeffer S, Loveday C, et al.: HIV results in the frame: Results confirmed. *Nature* 1995, 375:193.
- [18] Haase AT, Henry K, Zupancic M, Sedgewick G et al.: Quantitative image analysis of HIV-1 infection in lymphoid tissue. *Science* 1996, 274:985-989.
- [19] Crow JF, Kimura M: *An Introduction to Population Genetics Theory*, Harper & Row, NY, 1970.
- [20] Embretson J, Zupancic M, Beneke J, Till M, Wolinsky S, Ribas JL, Burke A, Haase AT: Analysis of human immunodeficiency virus-infected tissues by amplification and *in situ* hybridization reveals latent and permissive infections at single-cell resolution. *Proc. Natl. Acad. Sci. USA* 1993, 90:357-361.
- [21] McLean AR, Michie CA: *In vivo* estimates of division and death rates of human T lymphocytes. *Proc. Natl. Acad. Sci. USA* 1995, 92:3707-3711.
- [22] Goudsmit J, De Ronde A, Ho DD, Perelson AS: Human immunodeficiency virus fitness *in vivo*: Calculations based on a single zidovudine resistance mutation at codon 215 of reverse transcriptase. *J. Virol.* 1996, 70: 5662-5664.
- [23] Bonhoeffer S, Coffin JM, Nowak MA: HIV drug therapy and viral load (submitted).
- [24] Eron JJ, Benoit, Jemsek J, SL, MacArthur, RD, et al.: Treatment with lamivudine, zidovudine, or both in HIV-positive patients with 200-500 CD4+ cells per cubic millimeter. *N. Engl. J. Med.* 1995, 333:1662-1669.
- [25] Condra JH: Evidence for the existence of long-lived genetic reservoirs of HIV-1 in infected patients. *J. AIDS and Human Retroviruses* 1995, 10S3:S40.

- [26] Harrigan R, Stone C, Griffin P, Bloor S, Tisdale M, Larder B & CNA2001 Trial Team: Antiretroviral activity and resistance profile of the carbocyclic nucleoside HIV reverse transcriptase inhibitor 1592U89. *4th Conference on Retroviruses and Opportunistic Infections*, Washington, DC, January 23, 1997, Abstr. 15.
- [27] Stein D, Drusano G, Steigbigel R, Berry P, Mellors J, McMahon D, Teppler H, Hildebrand C, Nessly B, Chodakewitz J: Two year follow-up of patients treated with indinavir 800mg q8h. *4th Conference on Retroviruses and Opportunistic Infections*, Washington, DC, January 23, 1997, Abstr. 195.
- [28] Wong JK, Gunthard HF, Havlir DV, Haase AT, Zhang ZQ, Kwok S, Ignacio CC, Keating NA, Chodakewitz J, Emini E, Meibohm A, Jonas L, Richman DD: Reduction of HIV in blood and lymph nodes after potent antiretroviral therapy. *4th Conference on Retroviruses and Opportunistic Infections*, Washington, DC, January 26, 1997, Abstr. LB10.
- [29] Coffin JM: HIV population dynamics in vivo: Implications for genetic variation, pathogenesis, and therapy. *Science* 1995, 267: 483- 489.
- [30] Najera I, Holguin A, Quinones-Mateu ME *et al.*: *pol* Gene quasispecies of human immunodeficiency virus: Mutations associated with drug resistance in virus from patients undergoing no drug therapy. *J. Virol.* 1995, 69:23-31.
- [31] Whittle P: The outcome of a stochastic epidemic - a note on Bailey's paper. *Biometrika* 1955, 42:116-122.
- [32] De Boer RJ, Perelson AS: Target cell limited and immune control models of HIV infection: A comparison (submitted).

- [33] Phillips AN: Reduction of HIV concentration during acute infection: Independence from a specific immune response. *Science* 1996, 271:497-499.
- [34] Ho DD: Time to hit HIV, early and hard. *New England J. Med.* 1995, 333: 450-451.
- [35] Schapiro JM, Winters MA, Stewart F, Efron B, Norris J, Kozal MJ, Merigan TC: The effect of high-dose saquinavir on viral load and CD4<sup>+</sup> T-cell counts in HIV-infected patients. *Ann. Int. Med.* 1996, 124:1039-1050.
- [36] Havlir DV, Eastman S, Gamst A, Richman DD: Nevirapine-resistant human immunodeficiency virus: Kinetics of replication and estimated prevalence in untreated patients. *J. Virol.* 1996, 70:7894-7899.
- [37] Molla A, Korneyeva M, Gao Q, Vasavanonda S, Schipper PJ, Mo H *et.al.*: Ordered accumulation of mutations in HIV protease confers resistance to ritonavir. *Nature Medicine* 1996, 2:760-766.
- [38] Hirsch M, Meibohm A, Rawlins S, Leavitt R: Indinavir (IDV) in combination with zidovudine (ZDV) and lamivudine (3TC) in ZDV-experienced patients with CD4 cell counts  $\leq 50$  cells/mm<sup>3</sup>. *4th Conference on Retroviruses and Opportunistic Infections*, Washington, DC, January 26, 1997, Abstr. LB7.
- [39] Pialoux G, Fournier S, Moulignier A, Poveda JD, Clavel F, Dupont B: Central nervous system (CNS) as sanctuary of HIV-1 in a patient treated with AZT + 3TC + indinavir. *4th Conference on Retroviruses and Opportunistic Infections*, Washington, DC, January 23, 1997, Abstr. 233.

- [40] Lederman M, Connick E, Landay A, Kessler H, Kuritzkes D, St. Clair M *et al.*: Partial immune reconstitution after 12 weeks of HAART (AZT, 3TC, Ritonavir): preliminary results of ACTG 315. *4th Conference on Retroviruses and Opportunistic Infections*, Washington, DC, January 26, Abstr. LB13.
- [41] Mansky LM, Temin HM: Lower *in vivo* mutation rate of human immunodeficiency virus type 1 than that predicted from the fidelity of purified reverse transcriptase. *J. Virology* 1995, 69:5087-5094.
- [42] Moreno P, Rebollo MJ, Pulido F, Rubio R, Noreiga AR, Delgado R: Alveolar macrophages are not an important source of viral production in HIV-1 infected patients. *AIDS* 1996, 10:682-684.
- [43] Koenig S, Gendelman HE, Orenstein JM, *et al.*: Detection of AIDS virus in macrophages in brain tissue from AIDS patients with encephalopathy. *Science* 1986, 233:1089-1093.
- [44] Cao Y, Dieterich D, Thomas PA, Huang YX, Mirabile M, Ho DD: Identification and quantitation of HIV-1 in the liver of patients with AIDS. *AIDS* 1992, 6:65-70.
- [45] Ho DD, Rota TR, Hirsch MS: Infection of monocyte-macrophages by human T lymphotropic virus type III. *J. Clin. Invest.* 1986, 77:1712-1715.
- [46] Gartner S, Markovits P, Markovitz DM, Kaplan MH, Gallo RC, Popovic M: The role of mononuclear phagocytes in HTLV-III/LAV infection. *Science* 1986, 233:215-219.
- [47] van Furth R: *Inflammation: Basic Principles and Clinical Correlates*, Gallin JI, Goldstein IM, Snyderman S, eds., Raven Press, NY, 1992, 325-339.



## Appendix

**The model.** The equations describing our model are:

$$\dot{T}(t) = s + \lambda T(t) \left( 1 - \frac{T(t) + T_1^*(t) + T_2^*(t)}{T_{\max}} \right) - \mu T(t) - k_1(1-r_1)T(t)V_1^I(t) - k_2(1-r_2)T(t)V_2^I(t), \quad (14)$$

$$\dot{T}_1^*(t) = m_{11}k_1(1-r_1)T(t)V_1^I(t) + m_{21}k_2(1-r_2)T(t)V_2^I(t) - \delta_1 T_1^*(t), \quad (15)$$

$$\dot{T}_2^*(t) = m_{22}k_2(1-r_2)T(t)V_2^I(t) + m_{12}k_1(1-r_1)T(t)V_1^I(t) - \delta_2 T_2^*(t), \quad (16)$$

$$\dot{M}(t) = \lambda^M - \mu^M M(t) - k_1^M(1-r_1)M(t)V_1^I(t) - k_2^M(1-r_2)M(t)V_2^I(t), \quad (17)$$

$$\dot{M}_1^*(t) = m_{11}k_1^M(1-r_1)M(t)V_1^I(t) + m_{21}k_2^M(1-r_2)M(t)V_2^I(t) - \delta_1^M M_1^*(t), \quad (18)$$

$$\dot{M}_2^*(t) = m_{22}k_2^M(1-r_2)M(t)V_2^I(t) + m_{12}k_1^M(1-r_1)M(t)V_1^I(t) - \delta_2^M M_2^*(t), \quad (19)$$

$$\dot{V}_1^I(t) = (1-p_1)N_1\delta_1 T_1^*(t) + (1-p_1)N_1^M\delta_1^M M_1^*(t) - c_1 V_1^I(t), \quad (20)$$

$$\dot{V}_2^I(t) = (1-p_2)N_2\delta_2 T_2^*(t) + (1-p_2)N_2^M\delta_2^M M_2^*(t) - c_2 V_2^I(t), \quad (21)$$

$$\dot{V}_1(t) = N_1\delta_1 T_1^*(t) + N_1^M\delta_1^M M_1^*(t) - c_1 V_1(t), \quad (22)$$

$$\dot{V}_2(t) = N_2\delta_2 T_2^*(t) + p_2 N_2^M\delta_2^M M_2^*(t) - c_2 V_2(t). \quad (23)$$

Before therapy, we assume all virus is infectious and thus  $V_1^I(0) = V_1(0)$ ,  $V_2^I(0) = V_2(0)$ .

**Parameter values in Table 1.** The CD4<sup>+</sup> proliferation rate  $\lambda$  is set so that the rate of increase in the CD4<sup>+</sup> count under a powerful drug regimen corresponds to the rate of increase observed in [3] (an increase of 95 after six weeks). The logistic growth parameter  $T_{\max}$  is determined so that  $T(0)/T_{\max} = 0.40$ , which corresponds closely to the observed increase in the uninfected CD4<sup>+</sup> cell concentration under triple combination therapy in [1]. The T cell death rate  $\mu$  is consistent with a mean lifetime of two years (see [21] for estimates).

Estimates for  $\delta_i$  and  $\delta_i^M$  are from [3],  $c_i$  is from [7] and  $m_{12}$  and  $m_{21}$  are from [41]. The infectivity rate  $k_1$  is derived by simultaneously solving the three equations  $\lambda \left(1 - \frac{T_1 + T_1^*}{T_{\max}}\right) = \mu + k_1 V_1^I$ ,  $k_1 T_1 V_1^I = \delta_1 T_1^*$  and  $T + T_1^* = 180$  for the three unknowns  $k_1$ ,  $T$  and  $T_1^*$ , where the first two equations are the pre-treatment, no mutations, quasi-steady-state conditions for equations (14)-(15), and 180 is the average CD4<sup>+</sup> T cell count in Table 1 of [6]. The burst size  $N_1$  is derived from  $N_1 \delta_1 T_1^* = 0.96 c_1 V_1^I$ , which is the pre-treatment quasi-steady-state equation for (20), along with the estimate in [3] that about 96% of the virus is produced by infected CD4<sup>+</sup> T cells. The burst size  $N_2$  is set equal to  $0.99 N_1$ .

The identity of the long-lived compartment is not known. HIV-1 infected macrophages are present *in vivo* [42, 43, 44], and *in vitro* infected macrophages can continuously release virions for weeks [45, 46], making them a suitable candidate population. The lifespan of macrophages in different human tissues is not well characterized but is likely to be weeks to months. We thus choose  $\mu^M = 0.04 \text{ day}^{-1}$  consistent with a mean lifetime of 3-4 weeks. The parameters  $\lambda^M$ ,  $k_1^M$  and  $N_1^M$  are jointly derived from solving five equations - the three quasi-steady-state equations  $\lambda^M = \mu^M M + k_1^M M V_1^I$  (17),  $k_1^M M V_1^I = \delta_1^M M_1^*$  (18) and  $N_1^M \delta_1^M M_1^* = 0.04 c_1 V_1^I$  (20),  $M = 99 M_1^*$  (1% of the macrophages are infected) and  $N_1^M \delta_1^M = 0.1 N_1 \delta_1$  (the viral replication rate in infected macrophages is taken to be 10% of the replication rate of infected CD4<sup>+</sup> T cells) - for five unknowns:  $\lambda^M$ ,  $k_1^M$ ,  $N_1^M$ ,  $M$  and  $M_1^*$ . We also considered an alternative set of parameters that were derived by replacing the fifth equation,  $N_1^M \delta_1^M = 0.1 N_1 \delta_1$ , with the pre-infection steady-state for equation (17),  $\lambda^M = 1.43 \times 10^3 \mu^M = 57.2 \text{ cells/mm}^3/\text{day}$ , where  $1.43 \times 10^6 \text{ cells/mm}^3$  is an estimate for the total macrophage concentration [47]. The latter method causes a three-fold change in several of the macrophage parameters, but had only a negligible effect on the numerical solutions of the model as a whole. Similarly, sensitivity analysis reveals that the numerical solutions are highly insensitive to our crude estimates for  $\mu$  and  $\mu^M$ .

The values of the drug efficacy parameters  $r_i$  and  $p_i$  varied by run, and are described in the text. The mutation probabilities  $m_{12}$  and  $m_{21}$  have been chosen to correspond to the frequency of a single base change during HIV reverse transcription. For some drugs, such as 3TC and nevirapine, a particular single base change can render substantial drug resistance. For other drugs, multiple mutations may be needed or there may be multiple nucleotide positions at which mutation can confer resistance. In either event, this would need to be modeled by using a higher effective mutation probability,  $m_{12}$ . Sensitivity analysis shows that the model dynamics studied in the text are insensitive to any mutation probability  $m_{12}$  between  $10^{-5}$  and  $10^{-3}$ . If multiple, stepwise mutations are involved in generating resistance then the back mutation probability  $m_{21}$  would be expected to be smaller than the forward mutation probability  $m_{12}$ . Finally, the pre-treatment steady state was taken as the starting point of our model in the numerical runs.

**Post-treatment steady-state analysis.** We make a number of simplifying assumptions in our analysis. First, we assume that the drugs are 100% effective against the wild-type virus. Second, because the reverse mutation probability  $m_{21}$  is small, we assume that the wild-type virus will eventually be eradicated, and set  $T_1^* = M_1^* = V_1^I = V_1 = 0$  in steady state. We also ignore the  $T_2^*$  term in the logistic growth equation in (14). Finally, during our calculations, we set the value  $m_{22}$ , which is very close in value to one, equal to one.

By equations (16) and (19), we have  $\delta_2 T_2^* = k_2(1 - r_2)TV_2^I$  and  $\delta_2^M M_2^* = k_2^M(1 - r_2)MV_2^I$ . Substituting the right sides of these equations into (21) and cancelling the  $V_2^I$ 's yield

$$N_2 k_2 T + N_2^M k_2^M M = \frac{c_2}{1 - e_2}. \quad (24)$$

Equations (14) and (17) can be expressed as

$$V_2^I = \frac{\lambda(1 - \frac{T}{T_{\max}}) - \mu}{k_2(1 - r_2)} \quad \text{and} \quad V_2^I = \frac{\lambda^M - \mu^M M}{k_2^M(1 - r_2)M}. \quad (25)$$

Solving (24) for  $T$ , substituting this expression into the first equation in (25), and equating the right sides of the two equations in (25) lead to the following quadratic equation for  $M$ :

$$-\frac{\lambda N_2^M [k_2^M]^2}{T_{\max} N_2 k_2} M^2 + M \left[ \frac{\lambda k_2^M c_2}{T_{\max} N_2 k_2 (1 - e_2)} + (\mu k_2^M - \mu^M k_2 - \lambda k_2^M) \right] + \lambda^M k_2 = 0. \quad (26)$$

Equation (26) is only valid if  $V_2^I > 0$  and  $T > 0$ . By (25),  $V_2^I > 0$  if  $M < \lambda^M / \mu^M$ . Using the solution (the  $-\sqrt{\quad}$  solution is the useful root) to equation (26), this inequality after squaring both sides reduces to

$$1 - e_2 > \frac{c_2 \lambda}{T_{\max} N_2 k_2 (\lambda - \mu) + \lambda \lambda^M N_2^M k_2^M / \mu^M}. \quad (27)$$

By (24) and the solution to (26),  $T > 0$  if

$$1 - e_2 < \frac{c_2 [(\lambda - \mu) k_2^M + \mu^M k_2]}{\lambda^M N_2^M k_2 k_2^M}. \quad (28)$$

According to our parameter estimates, the first term in the denominator of (27) is several orders of magnitude larger than the second term. Hence, we ignore the second term, which gives rise to equation (2). It turns out that (2) is the exact eradication condition for the simpler model that omits long-lived cells.

We have three possible cases for the steady-state behavior. If (27) is violated then the virus is eradicated, and the steady-state solution is simply  $T = (\lambda - \mu) T_{\max} / \lambda$  and  $M = \lambda^M / \mu^M$ . If (27) and (28) are both satisfied then we get a steady-state solution in which the quantities  $T$ ,  $M$ ,  $T_2^*$ ,  $M_2^*$ ,  $V_2^I$  and  $V_2$  are all positive (for brevity's sake, we do not write out this solution). Finally, if (27) is satisfied and (28) is violated then the steady-state solution has virus but no uninfected CD4<sup>+</sup> cells. However, substituting the parameter values from Table 1 into the right side of (28) yields 25.7, and hence shows that the inequality is

satisfied for our default parameters. Further sensitivity analysis of (28) suggests that this inequality will always be satisfied, making it impossible to eliminate all uninfected CD4<sup>+</sup> T cells.

**Dynamic analysis.** If the drug regimen is 100% effective against the wild-type virus ( $r_1 = 1$ ,  $p_1 = 1$ ) and we ignore back mutation from mutant to wild-type ( $m_{21} = 0$ ) then the model can be solved in closed form, as in [3], to get

$$V_1(t) = \frac{N_1 \delta_1 T_1^*(0)}{c_1 - \delta_1} e^{-\delta_1 t} + \frac{N_1^M \delta_1^M M_1^*(0)}{c_1 - \delta_1^M} e^{-\delta_1^M t} + \left( V_1(0) - \frac{N_1 \delta_1 T_1^*(0)}{c_1 - \delta_1} - \frac{N_1^M \delta_1^M M_1^*(0)}{c_1 - \delta_1^M} \right) e^{-c_1 t}. \quad (29)$$

To obtain a closed form expression for the mutant virus we can relax the assumption of 100% drug efficacy against wild-type RT. If  $p_1 = 1$ , then  $V_1^I(t) = V_1^I(0)e^{-c_1 t}$ . Substituting into equations (14)-(23), ignoring the long-lived cells (i.e., assuming that  $M(t) = M_1^*(t) = M_2^*(t) = 0$ ), and for simplicity setting  $m_{22} = 1$  then

$$V_2(t) = \frac{N_2 \delta_2 \bar{C}_1}{c_2 + \theta_2} e^{\theta_2 t} + \frac{N_2 \delta_2 \bar{C}_2}{c_2 + \beta_2} e^{\beta_2 t} + \left( V_2(0) - \frac{N_2 \delta_2 \bar{C}_1}{c_2 + \theta_2} - \frac{N_2 \delta_2 \bar{C}_2}{c_2 + \beta_2} \right) e^{-c_2 t}, \quad (30)$$

where

$$\sigma = \sqrt{(c_2 - \delta_2)^2 + 4k_2 N_2 (1 - e_2) \delta_2 T(0)}, \quad (31)$$

$$\theta_2 = \frac{-c_2 - \delta_2 + \sigma}{2}, \quad \beta_2 = \frac{-c_2 - \delta_2 - \sigma}{2}, \quad (32)$$

$$\bar{C}_0 = m_{12} k_1 (1 - r_1) T(0) V_1^I(0), \quad (33)$$

$$\bar{C}_1 = \left( T_2^*(0) + \frac{\bar{C}_0}{c_1 + \theta_2} \right) \left( \frac{\sigma + c_2 - \delta_2}{2\sigma} \right) + \frac{V_2^I(0) k_2 (1 - r_2) T(0)}{\sigma}, \quad (34)$$

$$\bar{C}_2 = \left( T_2^*(0) + \frac{\bar{C}_0}{c_1 + \beta_2} \right) \left( \frac{\sigma - c_2 + \delta_2}{2\sigma} \right) - \frac{V_2^I(0) k_2 (1 - r_2) T(0)}{s}, \quad (35)$$

and we have assumed that  $c_1 = c_2$ .

Because the first term dominates the expression in (30), we investigate the constant  $\bar{C}_1$  to find its most significant factors. Notice that  $\bar{C}_0$  is proportional to the mutation probability  $m_{12}$ , whereas the last factor in (34) is independent of the mutation probability and depends only on the level of pre-existing mutant virus,  $V_2^I(0)$ . Substituting the values for  $m_{12}$  and  $k_1$  from Table 1 into (33) gives  $\bar{C}_0 = 1.2 \times 10^{-9}(1 - r_1)T(0)V_1^I(0)$ . Because  $\theta_2 \geq -\delta_2$ , a crude upper bound for the following term in (34) is

$$\frac{\bar{C}_0}{c_1 + \theta_2} \leq \frac{1.2 \times 10^{-9}(1 - r_1)T(0)V_1^I(0)}{c_1 - \delta_2} \leq \frac{1.2 \times 10^{-9}(10^3)(10^3)}{2.38} = 5.0 \times 10^{-4}, \quad (36)$$

where the second inequality in (36) assumes that  $T(0) \leq 1000$  cells/mm<sup>3</sup> and  $V_1^I(0) \leq 1000$  virions/ml and that  $c_1$  and  $\delta_2$  take on their values in Table 1. Hence, if  $T_2^*(0) \gg 5.0 \times 10^{-4}$  then the term in (36) will be negligible in (34).

Also, because  $\sigma + c_2 - \delta_2 \leq 2\sigma$  and  $r_1 > r_2$ , equation (36) implies that

$$\left( \frac{\bar{C}_0}{c_1 + \theta_2} \right) \left( \frac{\sigma + c_2 - \delta_2}{2\sigma} \right) \leq \frac{1.2 \times 10^{-9}(1 - r_2)T(0)V_1^I(0)}{c_1 - \delta_2}. \quad (37)$$

Substituting the values for  $k_2$  and  $\sigma$  from Table 1 into the last term of (34) yields

$$\left( \frac{\bar{C}_0}{c_1 + \theta_2} \right) \left( \frac{\sigma + c_2 - \delta_2}{2\sigma} \right) \leq \frac{V_2^I(0)k_2(1 - r_2)T(0)}{\sigma} \quad \text{if} \quad \frac{V_2^I(0)}{V_1^I(0)} \geq 3.65 \times 10^{-5}. \quad (38)$$

Therefore, if the fraction of virus that is mutant at time zero is significantly higher than  $3.6 \times 10^{-5}$  then the term in (36) will again be negligible in (34), and the concentration of mutant virus observed during therapy will mainly depend on the level of pre-existing mutant virus and depend little on the generation of drug resistant virus during therapy.